American Mineralogist, Volume 79, pages 692–699, 1994

Thermogravimetric study of the dehydration kinetics of talc

KUNAL BOSE,* JIBAMITRA GANGULY
Department of Geosciences, the University of Arizona, Tucson, Arizona 85721, U.S.A.

ABSTRACT

The dehydration kinetics of nearly pure talc, $(Mg_{0.99}Fe_{0.01})_3Si_4O_{10}(OH)_2$, and of pure synthetic talc to enstatite and SiO_2 was studied as a function of temperature between 777 and 977 °C and of grain size by thermogravimetry experiments. In the grain-size range of 15–1 μm, the rate of dehydration of talc increased with decreasing grain size, but further decrease of grain size did not significantly affect the dehydration rate. This may be caused by (1) clustering of the fine-grained particles as a result of surface charging, (2) a tradeoff between the positive effect of larger surface area and the negative effect of nucleating a larger number of product phases, or (3) both. The kinetic data can be adequately modeled by a second-order phenomenological rate law. The rate constant (k) for the size fraction of 10–15 μm of the natural talc follows an Arrhenian relation, $k = 1.98 \times 10^{14}\exp(-Q/RT)$/min, where the activation energy $Q = 372 \pm 7$ (σ) kJ/mol. Compared with talc of the same grain size, the synthetic talc was found to have a significantly faster dehydration rate. TEM images showed topotactic growth of enstatite on talc, with a concomitant formation of tridymite.

INTRODUCTION

The thermal decomposition of talc has received considerable attention over the past 30 years, primarily from the ceramic industry, since talc is used in a variety of industrial and consumer applications. In the context of planetary science and missions, experimental data on the reaction kinetics of talc and other phyllosilicates over a wide range of pressure are important for the quantitative analysis of the time-scale of formation of these minerals within the solar nebula (Fegley and Prinn, 1988) and other planetary environments, the depth and rate of release of H_2O into the mantle wedge during subduction processes (e.g., Delany and Helgeson, 1978; Peacock, 1990; Bose and Ganguly, 1993), and the evaluation of the feasibility of the extraction of H_2O from asteroidal and Martian rocks for use as fuel and life support for long-range planetary missions (Lewis and Lewis, 1987; Ganguly and Saxena, 1989).

There have been very few data so far on the dehydration kinetics of talc, the major emphasis of earlier works being on the structural changes associated with heating talc to high temperatures (e.g., Nakahira and Kato, 1964; Bošković et al., 1968; Brett et al., 1970; Daw et al., 1972; Konishi and Akai, 1991). Bošković et al. (1968) and Ward (1975) have carried out thermogravimetric studies of the dehydration kinetics of talc at 1 bar, whereas Greenwood (1963) has studied the kinetics of dehydration of talc at an H_2O pressure of 1 kbar in hydrothermal vessels. Under Greenwood's conditions, the decomposition of talc proceeded by means of an intermediate step involving the formation of anthophyllite according to talc → anthophyllite + quartz + H_2O → enstatite + quartz + H_2O. Greenwood found that his experimental data can be adequately modeled by assuming that each step follows a first-order rate law.

The work of Bošković et al. (1968) is unconvincing since, as emphasized by Ward (1975), they recorded only one or two points for a given temperature and made no attempt to distinguish between absorbed and structurally bound H_2O. Ward (1975) studied the kinetics of dehydration of what he called pure-grade talc between 827 and 887 °C at 1 bar, but he provided no chemical analysis for it. Assuming that talc breaks down to enstatite and quartz (+ vapor), which is the stable reaction at 1 bar, he treated the experimental data in terms of first-order reaction kinetics, but it is not clear how well a first-order rate law fitted the experimental data. Further, when the logarithms of rate constants given by Ward are plotted vs. inverse temperature (Fig. 1), a sudden break in slope at around 875 °C is apparent. This indicates that either there is a change in the dehydration mechanism above 875 °C or the first-order rate law is invalid over the studied temperature range. Although not stated by Ward (1975), his experimental activation enthalpy (or energy) fitted only the data between 826 and 872 °C. The five data at 881–886 °C were evidently rejected without any justification.

We have reinvestigated the dehydration kinetics of talc at 1 bar with the primary objective of testing the validity of Ward's data and determining the reaction mechanism. In addition, we have studied the behavior of both natural and synthetic talc, made a preliminary assessment of the

* Present address: Department of Geological and Geophysical Sciences, Princeton University, Princeton, New Jersey 08544, U.S.A.

0003–004X/94/0708–0692$02.00

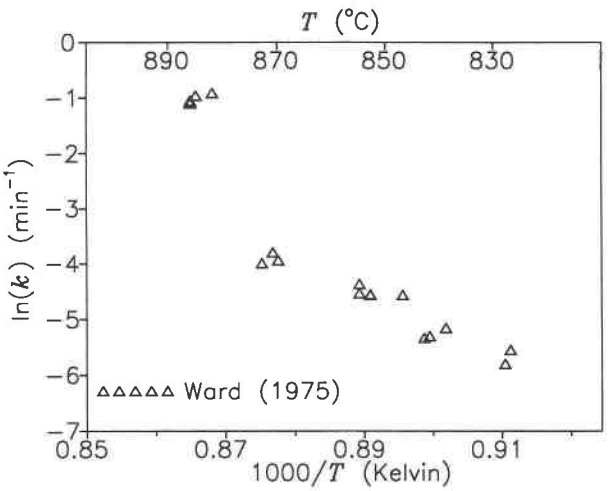

Fig. 1. Arrhenius plot of the dehydration rate constant (k) of talc in the temperature range 827–877 °C at 1 bar, as determined by Ward (1975). The cluster of five data points between 881 and 887 °C seems to have been ignored by Ward in the derivation of the kinetic parameters.

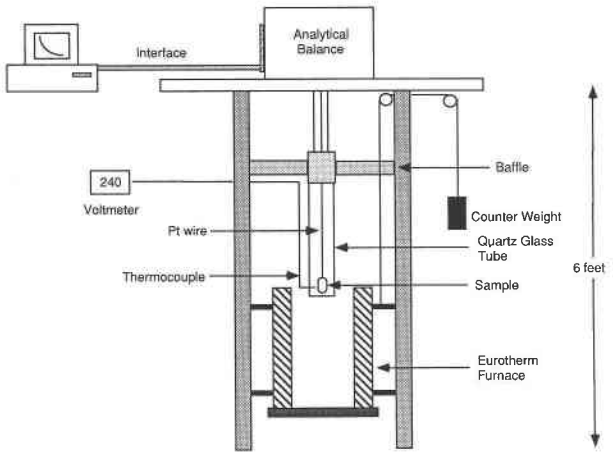

Fig. 2. Schematic illustration of the thermogravimetry apparatus built and used for the major portion of the present work. The thermocouple (Pt-Pt10%Rh) passes through an exterior quartz-glass tube, which is sealed to the one containing the sample.

effect of grain size on the dehydration kinetics, and tried to develop a general understanding of the kinetics of thermal decomposition of the phyllosilicates.

Experimental study

Starting materials

Natural talc. The natural talc used in this study came from Gouverneur, New York. Electron microprobe analysis of the sample showed it to be essentially a Mg end-member, with the chemical formula $(Mg_{0.99}Fe_{0.01})_3Si_4O_{10}(OH)_2$ (the analyzed oxide weight percents are SiO_2 = 62.89, Al_2O_3 = 0.019, MgO = 31.15, and FeO = 1.012). F, Cl, Ca, Ni, K, and Ti were below detection levels. A block of this material was cored by a diamond coring tool to obtain powders. This method was preferred over the more conventional crushing and grinding, since it minimized the sample strain that could affect the dehydration kinetics. A batch of sample with a grain size of 10–15 μm was separated by the centrifuge procedure described below. It was, however, necessary to grind this size fraction to obtain smaller grain sizes.

Three grain-size fractions, 10–15, 1–2, and <1 μm, were separated from the powdered material following the procedure of Starkey et al. (1984). The powder was sonified in distilled H_2O before spinning the suspension in an ultra centrifuge (IEC B-22M Programmable Centrifuge) at revolution rates and durations specified by Stokes's law of settling velocity for platy minerals, as derived by Hathaway (1956). Then the supernatant was decanted, and the procedure was repeated until a sufficient quantity of the desired size fraction was obtained. Optical and TEM examination confirmed the size fractions, and X-ray powder diffraction did not show any peaks other than those for talc. There was, however, significant peak broadening with decreasing grain size.

Synthetic talc. Talc was synthesized hydrothermally at 2 kbar and 640 °C from stoichiometric mixtures of MgO (99.99% Johnson Matthey Puratronic grade) and synthetic cristobalite, which were sealed with excess H_2O in Au capsules 0.5 in. in diameter. The duration of the synthesis experiments varied from 2 to 4 d, and each capsule contained about 150–200 mg of the mixture of MgO and cristobalite. Within the limit of resolution of X-ray diffractometer scans and the optical microscope, the synthesis products were single-phase talc. However, the XRD peaks of the synthetic talc were somewhat broader than those of the coarse-grained natural talc. Grain sizes of the synthetic talc varied between 1 and 2 μm.

The dehydration kinetics of talc was determined at 1 bar by thermogravimetric experiments, which involved monitoring the in-situ weight change of a sample of known initial weight as a function of temperature and time. The majority of the experiments were performed in a thermogravimetric apparatus (TGA) built in-house (Fig. 2). For reasons described below, a limited number of experiments were conducted in a microanalytical TGA at Princeton University. For experiments using the in-house apparatus, approximately 1 g of the talc with a size of 10–15 μm was placed in an alumina crucible, which was suspended by a Pt wire from the base of a digital Sauter analytical balance. The crucible assembly was enclosed by a quartz-glass tube with a Pt/Pt 10% Rh thermocouple immediately adjacent to, but not touching, the crucible. In order to ensure that the talc sample was free of hygroscopic moisture, a small auxiliary furnace, which was maintained at a temperature of ~130 °C, was placed around the quartz tube, and the weight loss of the sample was monitored until the weight became constant. At this stage, the auxiliary furnace was quickly removed, and the primary furnace, which was preheated to the temperature of the experiment, was raised such that the crucible was at the center of the hot spot (1.5 in. long) of the furnace.

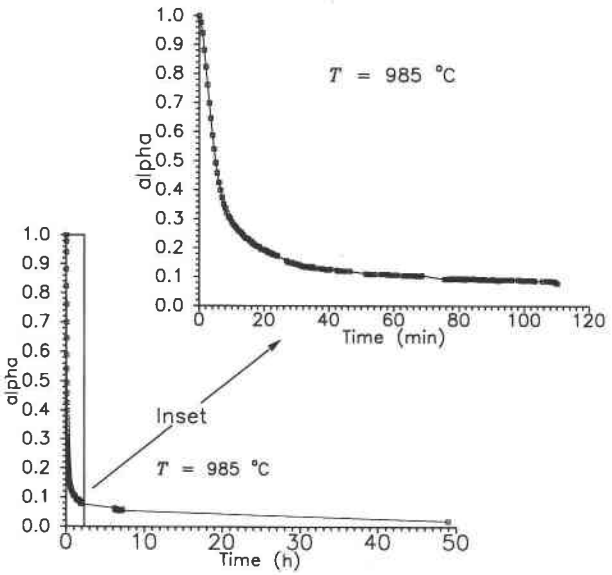

Fig. 3. Experimental verification of the theoretical anhydrous weight (w_∞), which has been used to calculate α in thermogravimetry experiments.

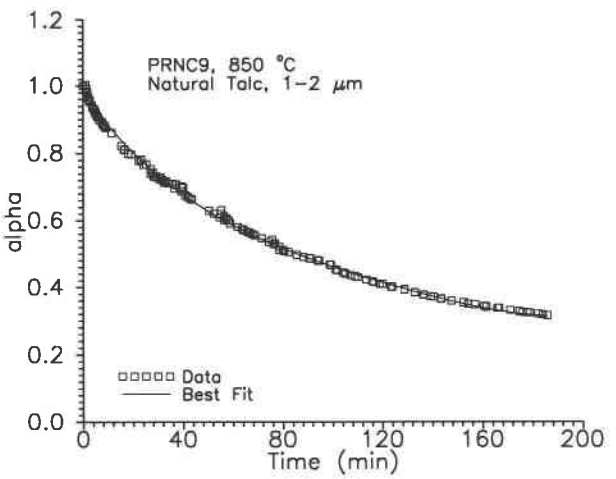

Fig. 4. Illustration of the polynomial fit to the data from thermogravimetry experiments.

It took about 2–3 min for the sample to come to thermal equilibrium, after which the fluctuation in sample temperature was <1 °C.

During an experiment, the suspension of the sample inside the furnace was supported by a needle passing through a small loop in the Pt wire attached to the sample crucible and resting on the top of the glass tube. The sample weight was determined at desired time intervals by linking the Pt wire to an extension support connected to the pan of the analytical balance through the bottom end. The connection between the balance and the loop was made by a rigid S-shaped hook of controlled length, and the supporting needle was removed so that the position of the sample inside the furnace was not disturbed. The output from the balance was sent through an analogue to digital converter to a personal computer, which monitored the weight change and also recorded the thermocouple emf output and time.

Initially, the sample was suspended directly from the analytical balance so that the weight change could be monitored continuously. However, this method had to be abandoned owing to the creep of the weight transducer, usually in experiments >45 min in duration. Thermal currents rising from the furnace also interfered with the determination of the weight change of the sample. However, this problem was nearly eliminated by placing a baffle at the bottom of the balance and adding a small fan directed at the top of the glass tube. A small aperture allowed free passage of the Pt suspension wire.

The maximum possible weight change of the sample after complete dehydration was about 4.75% of the initial weight, and there was about ±0.0001 g of statistical fluctuation in the weight as recorded by the balance. Thus, it was necessary to use at least 1 g of sample in each experiment so that the statistical fluctuations were small compared with the recorded weight changes. However, as it was very time consuming either to synthesize or to separate grain sizes of 1–2 and <1 μm from talc in sufficiently large quantities to conduct several experiments in our apparatus, experiments with these fine-grained materials were conducted in the microanalytical TGA (Setaram DSC-TGA 111) at Princeton University. This equipment can detect weight changes at the microgram level and thus requires only ~1 mg of sample for accurate measurements. However, as a disadvantage, the furnace could not be preheated to the desired experiment temperature. Thus, the sample was initially predried at 150 °C and inserted into the furnace, which was then heated to the desired experiment temperature. Although the predrying temperatures differed by 20 °C at the two laboratories, the weight change due to loss of hygroscopic moisture was the same (~0.5% of initial weight) after about 12 h. The time for the sample to reach a desired experiment temperature was much longer than in our in-house apparatus, and consequently a longer time-weight segment had to be subtracted from the total experiment duration, which constituted a potential source of error (see below). A second, and more serious, disadvantage of the microanalytical TGA was that the output from the weight transducer and the thermocouple was fed into a strip chart recorder. The absence of a digital recording device required manual reading of the weight loss vs. t data from the strip chart recorder, which introduced some random error and was also laborious.

To improve the resolution of the recorder data, the chart recorder was operated at a comparatively fast scan rate, resulting in hard-copy output more than 20 feet long in overnight experiments. These were then read off in sections 3 feet long in a digitizing tablet of 4 × 6 feet, interfaced to the VAX-8600 computer, using software that allowed writing the data in a digitized form onto a disk.

TABLE 1. Values of the parameters of the polynomial function used to fit α vs. t data in the thermogravimetry experiments ($\alpha = C_0 + C_1t + C_2t^2 + \cdots + C_nt^n$) and of the corresponding rate constant, k, at different temperatures

Expt.	Sample*	T (°C)	t (min)	n**	$C_0 \times 10$	$C_1 \times 10^4$	$C_2 \times 10^7$	$C_3 \times 10^9$	$C_4 \times 10^{11}$	$C_5 \times 10^9$	$C_6 \times 10^{12}$	Range of α	ln k/min
36NT775	N/10–15 μm	775	11042	200	9.42	−1.42	0.172	−73000				1.0–0.5	−9.75
38NT825	N/10–15 μm	825	1853	76	9.31	−13.5	21.1	−1.48	358.0			1.0–0.6	−7.8
				26	8.15	−4.95	2.53	−518.0				0.6–0.44	
PRNC8	S/1–2 μm	850	80	117	9.92	−734.3	38081.6	−119293	210511	1914.9	69.59	1.0–0.13	−2.472
PRNC9	N/1–2 μm	850	239	165	9.76	−95.026	602.8	−201.15	26.57			1.0–0.28	−4.47
PRNC10	N/0.5 μm	850	245	71	9.95	−108.38	813.54	325.96	50.75			1.0–0.26	−4.406
86EE876	N/10–15 μm	876	501	82	9.44	−35.0	143.0	−29.8	2.28			1.0–0.47	−6.19
73EE900	N/10–15 μm	900	1472	59	9.85	−127	1980	−1710.0	549.0			1.0–0.5	−5.3
				50	6.78	−16.8	23.4	−1.49	350.0			0.5–0.16	
PRNC3	N/1–2 μm	900	97.3	185	9.92	−426.4	12860.6	−22626.5	20230.4	−0.7042			
80EE925	N/10–15 μm	925	393	74	1.01	−249.0	6910	−10400	59.5			1.0–0.5	−4.36
				40	6.88	−32.4	73.4	−6.46				0.5–0.15	
77EE950	N/10–15 μm	950	130	73	10.1	−397.0	12200	−21600	21400	−1.09	2.25	1.0–0.25	−3.57
83EE977	N/10–15 μm	977	89	110	9.92	−360.0	8360.0	−97.8	4270			1.0–0.2	−3.03

* N = natural, S = synthetic.
** Number of data points.

Each scan was digitized at least ten times to reduce the error introduced by the manual tracing of the digitizing stylus (the mouse) over the chart recorder trace.

Experimental results

The weight change of talc vs. t was measured at seven temperatures between 775 and 977 °C for the grain-size fraction of 10–15 μm and at 850 and 900 °C for the two other size fractions (1–2 and <1 μm) of natural talc. In addition, the dehydration kinetics of the synthetic talc, which had a grain size of 1–2 μm, was also studied at 900 °C. For the presentation and analysis of experimental data, we define a parameter α as

$$\alpha = \frac{w_t - w_\infty}{w_0 - w_\infty} \quad (1)$$

where w_t is the weight of the sample at time t, and w_0 and w_∞ are its initial ($t = 0$) and anhydrous ($t = \infty$) weights, respectively. The parameter α varies between 1 at $t = 0$ and 0 at $t = \infty$ (i.e., when 100% of the reaction is completed).

The w_∞ was calculated from the stoichiometry of talc to be 4.75% of the initial weight of the sample. It was also checked experimentally by conducting a very long experiment at 985 °C (Fig. 3). The weight after 48 h was within 1.2% of the theoretical anhydrous weight. Thus, the theoretical value of w_∞ was accepted for calculating α from Equation 1. For the in-house experiments, w_0 was taken as the measured weight of the sample after introducing the sample into the hot spot of the furnace, allowing about 3 min for the stabilization of the system. This induction time was subtracted from the total duration of the experiment. For experiments performed in the microanalytical TGA at Princeton, a longer segment of data, covering, on the average, the first 10 min, was subtracted from the total data set.

The thermogravimetric data was smoothed by applying a polynomial fitting routine from the SPSS software package, and the polynomial fits were graphically inspected to ensure against ill- or overfitting the experimental data. Figure 4 illustrates a representative raw data set and the fitted polynomial function, which has the form $\alpha = C_0 + C_1t + C_2t^2 + \cdots + C_nt^n$. The parameters C_0–C_n are given in Table 1. To test the accuracy of the results of the thermogravimetry experiments, we have made independent experiments at 900 °C in our in-house TGA and in the microanalytical TGA at Princeton using the same stock of material. As illustrated in Figure 5, the results of these two independent experiments are in excellent agreement with one another.

The thermogravimetric data of the various size fractions of natural talc and the synthetic talc with a grain size of 1–2 μm at 900 °C are compared in Figure 6. It is clear that the dehydration kinetics of talc becomes faster with decreasing grain size in the range of 15–1 μm. Further decrease of grain size showed no noticeable effect on the dehydration kinetics. This could be caused by a trade-off between the enhancement effect of increasing surface area and the retardation effect associated with the development of a larger number of nucleation sites with the decreasing grain size. Alternatively, it could be the result of clustering of the very small particles caused by high electrostatic surface charging. As illustrated in Figure 6, the dehydration kinetics of synthetic talc is significantly faster than that of natural talc of the same grain size (1–2 μm). This implies a difference in the energetic properties of natural and synthetic materials, which was also reflected in the phase equilibrium studies (Bose and Ganguly, 1992; Bose, 1993), in that the natural talc was found to have a field of stability ~10–15 °C higher than that of the synthetic talc. The energetic difference is probably due to a higher defect density in the synthetic talc.

TRANSMISSION ELECTRON MICROSCOPIC STUDY: REACTION MECHANISM

We have carried out transmission electron microscopic (TEM) and selected-area electron diffraction (SAED) studies to characterize the products of the dehydration of talc and to understand the reaction mechanism. Indeed,

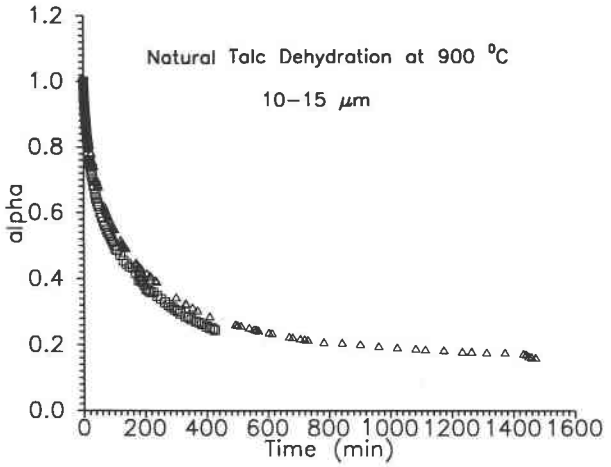

Fig. 5. Comparison of the data collected in thermogravimetry experiments at 900 °C using the apparatus illustrated in Fig. 2 (triangles) and a commercial microanalytical TGA unit, modified Setaram DSC-TGA 111 (squares).

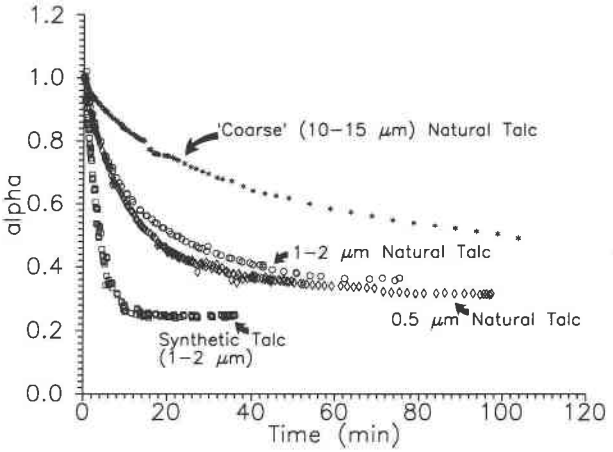

Fig. 6. Comparison of the thermogravimetry data at 900 °C for natural talc grain-size fractions of 10–15, 1–2, and 0.5 μm and synthetic talc grain-size fractions of 1–2 μm.

it was impossible to identify the products of dehydration by X-ray powder diffraction because of the samples' extremely fine grain size. Electron diffraction patterns from monomineralic mounts of talc, α quartz, tridymite, and orthorhombic enstatite were first indexed to serve as reference patterns for indexing the diffraction images of the products of the talc dehydration experiments. Crystallites, appearing as striations in the bright-field image (BFI) of dehydrated talc, were confirmed to be orthorhombic enstatite from indexing the corresponding SAED pattern, with the unit-cell parameters: a = 18.22, b = 8.8, c = 5.18 Å. Identification of the silica polymorph in the dehydrated product was difficult because of its amorphous to poorly crystallized nature and because of its lower abundance compared with enstatite. However, tridymite was identified in some SAED patterns obtained from dehydration products of longer experimental duration.

Superposition of SAED patterns of the unheated talc and the dehydrated product results in a composite SAED pattern as illustrated in Figure 7. It shows that the unit-cell axes of talc and enstatite are topotactically related according to

$$a_{talc}(5.28\ \text{Å}) \| c_{enst}(5.17\ \text{Å})$$

$$b_{talc}(9.17\ \text{Å}) \| b_{enst}(8.8\ \text{Å}).$$

These findings are consistent with the TEM observations of Santos and Yada (1988), Konishi and Akai (1991), and Bapst and Eberhart (1970), who noted in addition the topotactic relation of the $d(001)_{talc} \parallel a_{enst}$. Nakahira and Kato (1964) also arrived at the same conclusion from electron diffraction studies.

The observed topotactic relation between talc and enstatite permits the evaluation of the reaction mechanism involved in the dehydration of talc. Taylor (1962) distinguished "homogeneous" and "inhomogeneous" reaction mechanisms in the dehydroxylation or dehydration of layered hydrous silicates. In the "homogeneous" mechanism, loss of O atoms as H_2O molecules is uniform from all unit cells of the crystal, whereas in the "inhomogeneous" mechanism, which is also referred to as the heterogeneous nucleation and growth mechanism, there is no O loss from those parts of the crystal undergoing topotactic transformation. The heterogeneous mechanism involves (1) cation migrations, (2) formation and subsequent expulsion of H_2O molecules in a donor region, and (3) restructuring of the O framework within an acceptor region.

As schematically illustrated below, the transformation of talc to enstatite involves migration of $3Mg^{2+}$ cations from the donor to the acceptor region, in which enstatite is formed, accompanied by the countermigration of $6H^+$ to preserve charge balance.

Acceptor region	9Mg	12Si	36O	6H	→	12Mg	12Si	36O			
	↑			↓							
Donor region	3Mg	4Si	12O	2H	→	4Si	8O	+	8H	4O.	

It can be seen that no net transfer of O is involved in the formation of enstatite from one unit cell of talc, thus conforming to the "inhomogeneous" mechanism of Taylor (1962). The Mg^{2+} migrates to the acceptor region, in which the O framework is maintained virtually intact. Simultaneously, H_2O is lost from the donor region, which becomes silica rich. Given sufficient time, the amorphous silica crystallizes to tridymite.

Recently, Konishi and Akai (1991) have performed detailed high-resolution TEM studies to document the process of talc dehydration. Their study reinforced the above observations about dehydration mechanism of talc. In addition, they concluded that the dehydration of talc to enstatite and amorphous silica (with subsequent recrystallization to tridymite or cristobalite, depending on the temperature) involves depolymerization of the sheet

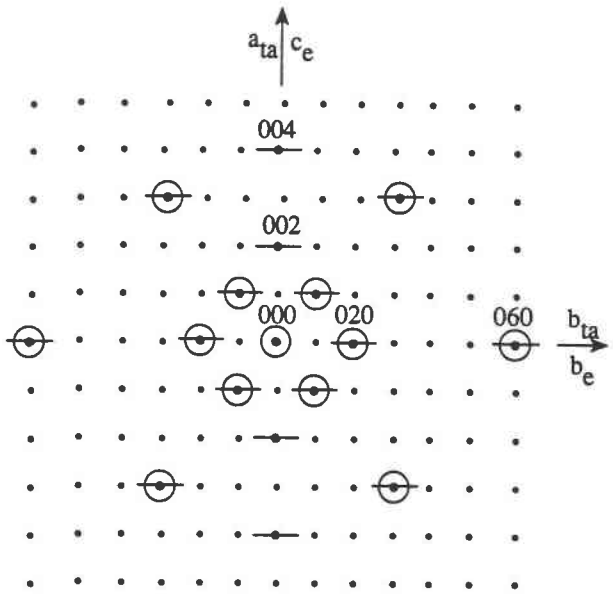

Fig. 7. Superimposition of the SAED patterns of talc and its dehydration products, showing topotactic growth of enstatite on talc.

structure to a disordered pyribole mixture of different chain widths, primarily single and double chains. They postulated that a pair of (010) faults with displacement of ½ (**a** + **c**) forms in adjacent double chains by breaking Si-O bonds. The unbonded Si^{4+} cations combine with OH^- by dehydroxylation, and new SiO_4 tetrahedral chains are formed. Mg^{2+} and H^+ migrate through the tunnel along the **c** axis of the double chain, with consequent formation of pyroxene between the two (010) faults (Konishi and Akai, 1991).

Phenomenological rate law and kinetic parameters

Under constant P-T conditions, a reaction rate may be phenomenologically expressed as

$$\text{rate} = -\frac{\partial C}{\partial t} = kC^n \qquad (2)$$

where C is the concentration of reactant per unit volume at time t, k is the rate constant, and n is the order of the reaction. This can be equivalently expressed in terms of any physically measurable property of the reactant that is proportional to its concentration (cf. Margerison, 1969; Moore and Pearson, 1981). In terms of α, Equation 2 reduces to

$$\text{rate} = -\frac{\partial \alpha}{\partial t} = k\alpha^n. \qquad (3)$$

The phenomenological analysis of kinetic data involves comparison of the data with an explicit form (i.e., with specific value of n) of Equation 2 or 3. Computationally, an integrated form of these equations is easier to manipulate than the differential form, since slight perturbations in the raw data (sampling errors) can cause large changes

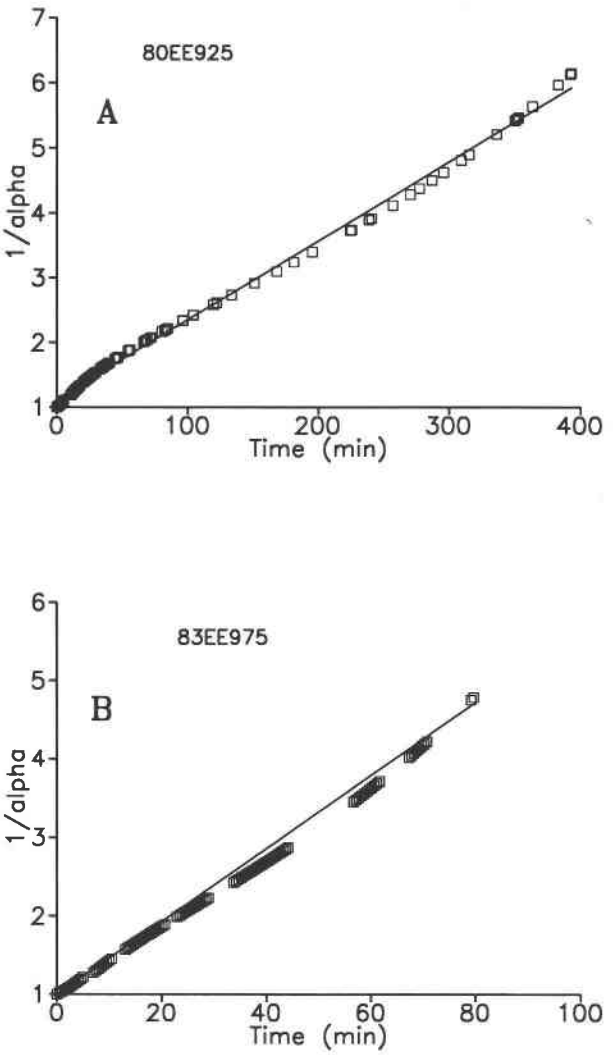

Fig. 8. Illustration of the quality of fit of the experimental data to a second-order rate law ($1/\alpha = 1 + kt$) for natural talc with a grain-size fraction of 10–15 μm at (**A**) 925 °C ($r^2 = 0.996$) and (**B**) 850 °C ($r^2 = 0.99$).

in the derivative between adjacent points. It is found that the thermogravimetry data can be described very well ($r^2 = 0.98$–0.99) by the integrated form of Equation 3 with $n = 2$:

$$\frac{1}{\alpha} = \frac{1}{\alpha_0} + kt \qquad (4)$$

which represents an integrated *second-order* rate expression. The data were analyzed in terms of $1/\alpha$ vs. t by linear regression using the SPSS software package, with the constraint that $\alpha = 1$ at $t = 0$. Figure 8 shows the linear dependence of $1/\alpha$ vs. t for two experiments using natural talc, one for a grain size of 10–15 μm at 925 °C, and the other for a grain size of 1–2 μm at 850 °C.

The thermogravimetric data for the various size fractions of synthetic and natural talc are summarized in Table

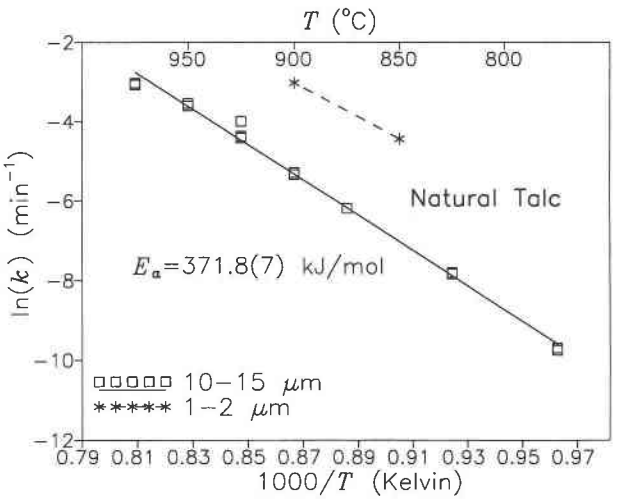

Fig. 9. Arrhenius plot of the rate constant for the dehydration of talc (retrieved by using a second-order rate law) in the temperature range 725–977 °C. Overlapping squares (thick outlines) represent pairs of data points.

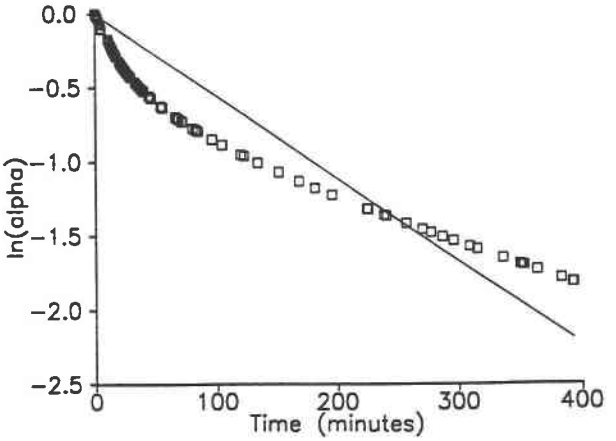

Fig. 10. Illustration of the poor fit of the experimental data used in Fig. 8A to a first-order rate law ($\ln \alpha = \ln \alpha_0 - kt$) proposed by Ward (1975) for the dehydration kinetics of talc.

1. Sufficient kinetic data are available for the grain-size fraction of 10–15 μm of natural talc to enable formulation of the temperature dependence of the dehydration rate constant. Within the experimental temperature range of 775–975 °C, the k vs. T data for the size fraction 10–15 μm can be described by an Arrhenian relation,

$$k = 1.98(10^{14})e^{\frac{-Q}{RT}}/\text{min} \quad (5)$$

where the activation energy Q = 372 ± 7 kJ/mol, the error representing ±1σ uncertainty. The Arrhenius fit to the experimental data for the size fraction of 10–15 μm is illustrated in Figure 9, along with the two values for the natural talc with a grain size of 1–2 μm.

Discussion

The second-order rate law for the decomposition of talc at 1 bar to enstatite + quartz + H_2O, derived from the results of our thermogravimetry experiments, is in contrast to the work of Ward (1975), who suggested a first-order rate law for the same reaction at 1 bar. Figure 10 shows a comparison of the same experimental data sets as in Figure 8 with the first-order rate law, $\ln \alpha(t) = \ln \alpha (t = 0) - kt$. It is evident that the latter fails to fit our data. Further, the Arrhenius relation illustrated in Figure 9 does not support the sudden change in activation energy between 871 and 875 °C (Fig. 1) that is implied by the data of Ward (1975).

As discussed earlier, Greenwood (1963) found that the experimental data on the decomposition of talc to enstatite + quartz at 1 kbar, which involved the formation and breakdown of anthophyllite as an intermediate step, can be adequately modeled by a first-order rate law. The reaction talc ⇌ anthophyllite + quartz + H_2O is stable between a few hundred bars and 12 kbar (Evans and Guggenheim, 1988). It is noteworthy that, according to our experimental data, the direct breakdown of talc to enstatite + quartz at 1 bar follows a second-order rate law. Further, Greenwood (1963) determined an activation energy of 590 ± 75 kJ/mol for the decomposition of talc to enstatite + quartz by means of anthophyllite, a value much larger than that determined in our work (372 ± 7 kJ/mol) for the direct transformation of talc to enstatite + quartz at 1 bar. It is not unlikely that the decomposition of talc above the field of anthophyllite stability, such as in subduction-zone environments, might follow a second-order rate law with an activation energy significantly lower than that determined by Greenwood.

The dehydration kinetics of several other phyllosilicates have been studied earlier. These include serpentine (Ball and Taylor, 1963; Wegner and Ernst, 1983), muscovite (Nicol, 1964), pyrophyllite (Brindley, 1975), and kaolinite (Brett et al., 1970). It appears, from a survey of these data along with our data for talc, that the dehydration mechanism of hydrous phyllosilicates as a class follows a heterogeneous nucleation and growth mechanism, with a narrow activation energy range of 325–400 kJ/mol.

Acknowledgments

The TEM pictures were taken and indexed by Supapan Seraphin and H. Makihara of the Department of Material Sciences, University of Arizona, to whom we express our gratitude. We are grateful to Alexandra Navrotsky, for allowing access to the microanalytical TGA in her laboratory, and to Steve Sorenson and Denis Norton, for allowing the use of the digitizing tablet and supporting software and for showing us how to use it. The talc sample was provided by Eric Essene. Thanks are due to Randy Cygan and an anonymous reviewer for careful and constructive reviews of the manuscript. This research was supported by grant no. NAGW-1332 from the University of Arizona–NASA Center for the Utilization of Local Planetary Resources.

References cited

Ball, M.C., and Taylor, H.F.W. (1963) The dehydration of chrysotile in air and under hydrothermal conditions. Mineralogical Magazine, 33, 467–481.

Bapst, G., and Eberhart, J.P. (1970) Transformation of talc to $MgSiO_3$. Bulletin du Groupe français des Argiles, 22, 17–23.

Bose, K. (1993) Equilibrium and kinetic studies in the system MgO-SiO_2-H_2O. Ph.D. thesis, University of Arizona, Tucson, Arizona.

Bose, K., and Ganguly, J. (1992) High pressure phase equilibria in the system MgO-SiO_2-H_2O: Quartz-coesite revisited and dehydration of talc (abs.). Eos, 73, 618–619.

——— (1993) Stability of talc at high pressures: Experimental determination, retrieval of thermodynamic properties, and applications to subduction processes. Geological Society of America Abstracts with Programs, 25, 213–214.

Bošković, S.B., Gašić, M.Č., Nikolić, V.S., and Ristić, M.M. (1968) The structural changes of talc during heating. Proceedings of the British Ceramic Society, 10, 1–12.

Brett, N.H., MacKenzie, K.J.D., and Sharp, J.H. (1970) The thermal decomposition of hydrous layer silicates and their related hydroxides. Chemical Society of London Quarterly Reviews, 24, 185–207.

Brindley, G.W. (1975) Thermal transformations of clays and layer silicates. Proceedings of the International Clay Conference, Mexico City, Mexico, 1975, p. 119–129. Applied Publishing, Wilmette, Illinois.

Daw, J.D., Nicholson, P.S., and Amber, J.D. (1972) Inhomogeneous dehydroxylation of talc. Journal of the American Ceramic Society, 55, 149–151.

Delany, J.M., and Helgeson, H.C. (1978) Calculation of the thermodynamic consequences of dehydration in subducting oceanic crust to 100 kb and >800 °C. American Journal of Science, 278, 638–686.

Evans, B.W., and Guggenheim, S. (1988) Talc, pyrophyllite and related minerals. Mineralogical Society of America Reviews in Mineralogy, 19, 225–294.

Fegley, B., Jr., and Prinn, R.G. (1988) Solar nebula chemistry: Implications for volatiles in the solar system. In H.A. Weaver, F. Paresce, and L. Danley, Eds., The formation and evolution of planetary systems, p. 171–211. Cambridge University Press, Cambridge, U.K.

Ganguly, J., and Saxena, S.K. (1989) Theoretical predictions of volatile abundances and volatile bearing phases in carbonaceous chondrites. In B. Faughnan and G. Maryniak, Eds., Space manufacturing 7: Space resources to improve life on Earth, p. 97–108. American Institute of Aeronautics and Astronautics, Washington, DC.

Greenwood, H.J. (1963) Synthesis and stability of anthophyllite. Journal of Petrology, 4, part 3, 37–51.

Hathaway, J.C. (1956) Procedure for clay mineral analyses used in the sedimentary petrology laboratory of the U.S. Geological Survey. Clay Minerals Bulletin, 3, 8–13.

Konishi, H., and Akai, J. (1991) Depolymerized pyribole structures derived from talc by heating. Physics and Chemistry of Minerals, 17, 569–582.

Lewis, J.S., and Lewis, R.A. (1987) Space resources, 418 p. Columbia University Press, New York.

Margerison, D. (1969) The treatment of experimental data. In C.H. Bamford and C.F.H. Tipper, Eds., Comprehensive chemical kinetics, vol. 1, p. 343–421. Elsevier, Amsterdam.

Moore, J.W., and Pearson, R.G. (1981) Kinetics and mechanism (3rd edition), 455 p. Wiley, New York.

Nakahira, M., and Kato, T. (1964) Thermal transformation of pyrophyllite and talc as revealed by X-ray and electron diffraction studies. Clays and Clay Minerals, 12, 21–27.

Nicol, A.W. (1964) Topotactic transformation of muscovite under mild hydrothermal conditions. Clays and Clay Minerals, 12, 11–19.

Peacock, S.M. (1990) Fluid processes in subduction zones. Science, 248, 329–337.

Santos, H.deS., and Yada, K. (1988) Thermal transformation of talc as studied by electron-optical methods. Clays and Clay Minerals, 36(4), 289–297.

Starkey, H.C., Blackmon, P.D., and Hauff, P.L. (1984) The routine mineralogical analysis of clay bearing samples. U.S. Geological Survey Bulletin, 1563, 32 p.

Taylor, H.F.W. (1962) Homogeneous and inhomogeneous mechanisms in the dehydroxylation of minerals. Clay Minerals Bulletin, 28, vol. 5, 45–55.

Ward, J.R. (1975) Kinetics of talc dehydroxylation. Thermochimica Acta, 13, 7–14.

Wegner, W.E., and Ernst, W.G. (1983) Experimentally determined hydration and dehydration reaction rates in the system MgO-SiO_2-H_2O. American Journal of Science, 283A, 151–180.

Manuscript received August 30, 1993
Manuscript accepted February 18, 1994